Evaluating the Impacts of Climate Change on the Stream Flow Events in Range of Scale of Watersheds, in the Upper Blue Nile Basin

Gerawork F. Mulu[1], Mamaru A. Moges[2](✉), and Bayu G. Bihonegn[1]

[1] Department of Hydraulic and Water Resource Engineering, Kombolcha Institute of Technology, Wollo University, Dessie, Ethiopia
geru302@gmail.com

[2] Faculty of Civil and Water Resources Engineering, Bahir Dar Technology Institute, Bahir Dar University, Bahir Dar, Ethiopia
mamarumoges@gmail.com

Abstract. The main focus on three watersheds in the upper Blue Nile. The study used the Representative concentration pathway (RCP) climate model scenarios with 50 km resolution. The CORDEX-Africa model output of RCP2.6 and RCP8.5 scenarios were used. The Parameter Efficient Semi Distributed Water Balance model (PED-WM) was calibrated and validated to project the climate change impacts on the stream flow events. The future climate projection results were presented by dividing in to three future time horizons of 2030s (2021–2040), 2060s (2051–2070) and 2090s (2081–2100). The bias corrected maximum and minimum temperature increases in all months and seasons in the selected watersheds. The change in magnitude in RCP8.5 emission was higher than RCP2.6 scenario. The study resulted considerable average monthly, seasonal and annual precipitation change variability in magnitude and direction. In 2030s, the average annual Stream flow projection decreases up to −32.18% for RCP2.6 and up to −19.44% for RCP8.5 scenarios. In 2060s also the average annual stream flow decreases by −12.3% and −32.18% for RCP2.6 and RCP8.5 emission scenarios, respectively. Similarly, in 2090 s, the average annual Stream flow change decreases by −20.67 and −51.78% for RCP2.6 and RCP8.5 respectively. For the future time horizon, the maximum Stream flow changes in wide range from (−56.4 to 81.1%) and minimum flow from (−61.72 to 8.17%) in both RCP2.6 and RCP8.5.

Keywords: Blue Nile · CORDEX · RCP · Scenario · PED-WM

1 Introduction

For centuries, the environment has been influenced by human beings. In any case, it is just since the start of the modern unrest that the effect of human exercises has started to reach out to a worldwide scale [1]. Today, environmental issue turns into the greatest worry of humankind as an outcome of logical proof about the expanding centralization of ozone harming substances in the environment and the changing atmosphere of the Earth. All

N. G. Habtu et al. (Eds.): ICAST 2019, LNICST 308, pp. 169–192, 2020.
https://doi.org/10.1007/978-3-030-43690-2_12

around, temperature is expanding and the sum and appropriation of precipitation is being changed [2]. The effect of environmental change on water assets are the most critical research plan in overall dimension [3]. This change in climate causes a significant impact on the water resource by disturbing the normal hydrological processes. Future change in overall flow of magnitude, variability and timing of the main flow event are among the most frequently cited hydrological issues. According to the International Panel on Climate Change (IPCC) Scientific Assessment Report, the increased concentrations of CO_2 and other greenhouse gases in the atmosphere since 1750 have been comprised the prominent causes of climate change. The combined land and sea surface temperature in worldwide has expanded by 0.85 °C (0.65 °C to 1.06 °C), over the period from 1880 to 2012. Crosswise over a lot of Africa, for instance, projections dependent on the high Representative Concentration Pathway (RCP), suggests that a mean yearly temperature peak will occur in mid-century and could riches 3 °C and 6 °C and before the finish of the 21st century and ocean level rise up to 100 cm by 2100 [4].

The IPCC finding indicated that in developing countries, such as Ethiopia there will be more vulnerability to climate change. This is due to less flexibility to adjust the economic structure and being largely dependent on agriculture, the impact of climate change has far reach implications in Ethiopia. The upper Blue Nile Basin is one of the largest basins in the country with high population pressure, degradation of land and highly dependent on agricultural economy. The increase in population growth, economic development and climate change have been proven by IPCC, 2007 [5] to cause rise in water demand, necessity of improving flood protection system and drought (water scarcity). The Upper Blue Nile River catchments are the main sources for the Blue Nile River basin and their water resources are an important input for the different water development projects and the livelihood support of the people in the basin.

The climate in this basin is variable from region to region. Due to variable climatic regions this impact might not be similar throughout the upper Blue Nile basin. Some studies on climate change impacts on the Upper Blue Nile region was conducted using fourth assessment report [6–11]. Most the above studies focusing on annual and seasonal total precipitation and stream flow. Studies that considered extreme conditions are limited. However, the results of these investigations are often divergent and inconsistent. This study differs from the previous, the study used (i) Parameter Efficient semi Distributed (PED-W) hydrological saturation excess water balance model which was tested for Ethiopian highlands having monsoonal climate (ii) to dated Representative Concentration Pathway (RCP) scenarios and (iii) different scale of ranges of watersheds. The study of the changes of hydro-climatic extreme events occurring at local and regional levels using to dated RCP scenario was necessary in order to provide valuable information which assists all stakeholders and policy makers to build up an innovative thinking on water resource availability and productivities as response to climate change risks and make appropriate decisions and to adapt the current situation and changes in water resources that might occur due to climate change. Gilgel Abbay, Temcha and Anjeni watersheds are the selected watersheds in the Upper Blue Nile basin in which currently, different multipurpose water resources development projects are proposed and constructed in the river basin. So, it is critical to determine the hydrological responses to climate change for the sustainability of the projects and looking for the possible mitigation measures.

The objective of this study is to evaluate the impacts of climate change on stream flow events in different ranges of watersheds in the upper Blue Nile river basin using PED-W model. The precipitation and temperature scenarios have been bias corrected to the fine resolution required by the hydrological model from RCM using change factor bias correction method.

2 Description of the Study Area

The locations of the selected catchments are lie in the upper Blue Nile basin, between 7°45′ and 12°45′ N, and 34°05′ and 39°45′ E.

Anjeni watershed is situated about longitude of 37°31′ E and latitude of 10°40′ N, in the Northern part of Ethiopia. It is bordered by the DebreMarkos-Bahir Dar road, 15 km north of Dembecha town on the rural road to Feres Bet and 65 km north-west of DebreMarkos [12–14] and the size of the hydrological catchment is about 113.4 ha. Temcha watershed is located in the Amhara Region near Dembecha town. It lies in between 10°23′ to 10°41′ N latitude and 37°16′ to 37°45′ E longitude with an average elevation of 2083 m and lies 350 km NW of Addis Ababa and have an area of 406 km^2.

Gilgel Abbay watershed which is found in Tana basin and lies between (10°56′ to 11°51′ N) latitude and (36°44′ to 37°23′ E) longitude. Gilgel Abbay catchment is the biggest of the four main sub-basins of Lake Tana Basin. It depletes the southern part of Lake Tana basin to perennially feed lake tan River which empties itself in Lake Tana.

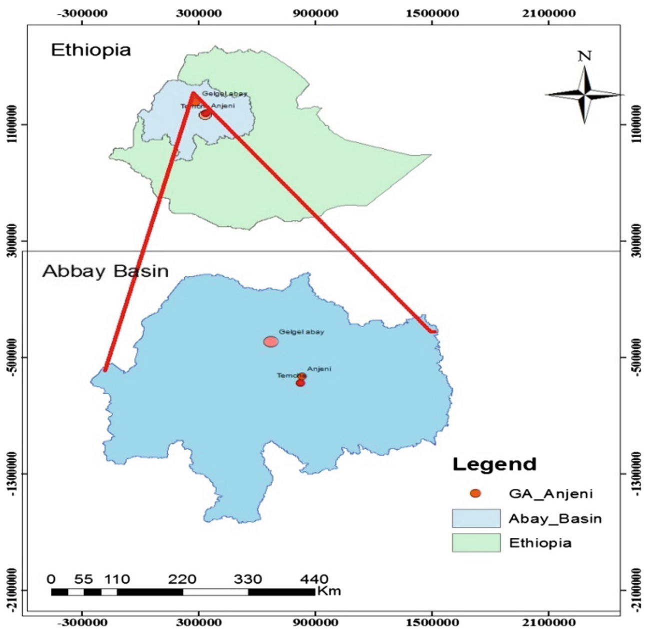

Fig. 1. Location of map of the study area

Being the main tributary of Lake Tana, Gilgel Abbay River originates from springs, considered as sacred water by the local people, located at an elevation 2750 m a.m.s.l near Mt. Gish. The hydrological catchment covers an area of 1650 km^2 (Fig. 1).

3 Methodology

3.1 Data Sources and Availability

Meteorological data collected from National Metrological Station Agency (NMSA), in Bahir Dar branch. SRTM 30 m × 30 m DEM data was used as an input data for Arc GIS software for catchment delineation. Hydrological data (stream flow) for the selected rivers in the upper Blue Nile River basin were used for model calibration and validation. These data were collected from the Ethiopia Ministry of Water Energy and Water Resources (MoWIE).

3.2 Climate Scenario Data

The future Precipitation and temperature (maximum and minimum) CORDEX-Africa GCM output 0.5 degree by 0.5 degree resolution RCP2.6 and RCP8.5 data was downloaded from Earth System Grid Federation (ESGF) Website http://www.csag.uct.ac.za/cordex-africa. Daily precipitation and temperature are taken from a set of simulations (historical and scenario) conducted with the CORDEX-Africa climate model. The projection depends on the bases of the new greenhouse gas concentration emission of representative concentration pathways (RCP).

The climate data ranges from 1^{st} January 1976 until 31^{st} December 2005 as historical period and for RCP4.5 and RCP8.5 which include data from 1^{st} January 2006 until 31^{st} December 2100. The temperature and precipitation data were bias corrected using change factor method developed by [15].

3.3 Potential Evapotranspiration (PET)

There are a number of methods to estimate potential evapotranspiration. The estimation methods vary based on climatic variables required for calculation. These are temperature-based method which use only temperature and sometimes day length; radiation-based method which uses net radiation and temperature and other formulas like [16] where it requires both temperature and net radiation and other climatic variables like wind speed and relative humidity. In area where there are data scarce, temperature method such as Enku's are required. For this specific study temperature based Enku's simple temperature method [17] is adopted to calculate the daily potential evaporation during model calibration and validation.

$$ET_o = \frac{(T\max)^n}{K} \tag{1}$$

Where, ET_o is the reference evapotranspiration (mm day^{-1}), n is 2.5 which can be calibrated for local conditions, k is Coefficient which can be calibrated for local conditions. The coefficient, k could be approximated as $k = 48 * T_{mm} - 330$ where T_{mm} is the mean annual maximum temperature.

3.4 Parameter Efficient Semi Distributed Watershed (PED-W) Model

The Parameter Efficient semi Distributed watershed (PED-W) model is a conceptual semi-distributed watershed model for continuous daily time step simulation of catchment runoff [18]. The model input requirement for PED model are daily rainfall, evapotranspiration, the areal fraction, maximum storage for each zone and the inter flow and base flow time. In PED-W the watershed is subdivided into three zones, degraded hill slope with little or no soil cover and the two runoff producing zone distinguished as the bottom lands that potentially saturate in the rainy monsoon phase, and one zone which contributes interflow and base flow of the watershed is permeable hill slope zone. PED-W model used to simulate future stream flow. The hydrological model was calibrated and validated using observed stream flow data of the selected watersheds in the basin. The model was selected because of its simplicity, suitability for monsoonal climate, easily availability, and widely acceptance.

PED-W Model Calibration and Validation

The PED-W model was calibrated manually, first by fitting the runoff volumes and followed by calibrating the shape of the hydrograph. The data record of 1990–2000, 1986–1994 and 1986–1994 was used for calibration for Gilgel Abbay, Temcha and Anjeni respectively. The calibrated model was validated using the independent set of observed from 2001–2005, 1996–1998 and 1995–1998 for Gilgel Abbay, Temcha and Anjeni respectively.

PED-W Model Performance Criteria

The performance of the model was evaluated by the Nash–Sutcliffe efficiency, (NSE) [19] Root Mean Square, RMS and Coefficient of Determination (R^2). NSE is a standardized measurement that determines the relative magnitude of the residual variance compared to the measured observed flow variance. NSE ranges from negative infinite to 1. Generally, NSE value between 0.6 and 0.8 indicates fair to good performance and when NSE is above 0.8 a model is said to be very good [20].

$$NSE = 1 - \frac{\sum_{i=1}^{n} (Q_{oi} - Q_{si})^2}{\sum_{i=1}^{n} (Q_{oi} - Q_o)^2}$$

Where Q_{oi} = observed discharge, Q_{si} = simulated discharge, Q_o = mean of observed discharge.

RMSE determines the degree to which the model predictions deviate from the observed data. The model efficiency (ENS) values ranges from 1.0 (best) to negative infinity.

R^2 is indicates how the simulated data correlates to the observed values of data. The range of R^2 is extends from 0 (unacceptable) to 1(best).

$$R^2 = \frac{\left[\sum_{i=1}^{n} (Q_{si} - \overline{Q}_s)(Q_{oi} - \overline{Q}_o\right]^2}{\sum\left[Q_{si} - \overline{Q}_s\right]\sum\left[Q_{oi} - \overline{Q}_o\right]}$$

Where Q_{si} is the simulated value, Q_{oi} is the measured values, $\overline{Q}_s$ is the average simulated value, $\overline{Q}_o$ is the average measured value.

4 Results and Discussion

In this investigation, 0.5 degree by 0.5-degree grid resolution CORDEX-Africa bias corrected GCM model outputs based on RCP2.6 and RCP8.5 emission scenarios for three watersheds in the upper Blue Nile Basin used for analysis. Period from 1976–2005 taken as a base period and three future periods considered for impact investigation of 2030s (2021–2041), 2060s (2051–2070) and 2090s (2081–2100). In order to check the exactness replication of the multimodal prediction for the basin the CORDEX-Africa model historical climate data output compared against observation data for each catchment. The mean monthly precipitation, maximum and minimum temperature observed (1986–2005) and GCMs (1976–2005) compared for three catchments (Anjeni, Temcha and Gilgel Abbay) for Upper Blue Nile Basin. All changes in projected climate variables under this study have been evaluated bias corrected base line climate variable. The climate change analysis was first by evaluating climate variables with corrected base line period. Secondly stream flow change evaluation due to climate change by simulating discharge using base line period and projected climate variables.

4.1 Historical GCMs Output Comparison with Observed Data

The raw RCM (CORDEX-Africa) out of long term daily and mean monthly precipitation and temperature indicated that there is relatively good agreement in trend and pattern with the observed data. The daily and monthly correlation of the selected grid point RCM model out puts with the observed station data was in the range of (0.35–0.44) and (0.85–0.90) respectively over the historical period. The observed data indicated that mean annual precipitation over the Gilgel Abbay watershed was 1380.92, 1490.25 and 2300 mm/year for Bahir Dar, Dangila and Injibara respectively, while the CORDEX-Africa climate model output have 2220.75 mm/year. For Anjeni and Temcha watersheds the mean annual observed precipitation was 1608 and 1393 mm/year and climate model output 1385.96 and 1385.96 mm/year respectively. The model out have little variation with the observed data, therefore the bias correction was inevitable to decrease the discrepancy between cordex output and observed data. The outputs of CORDEX model maximum and minimum temperature data have daily and monthly correlations of (0.53–0.63) and (0.85–0.90) over the historical period with observed respectively. From the observed records, average maximum temperatures 26.8 °C and 24.4 °C and average minimum temperatures 12.27 °C and, 8.5 °C for Bahir Dar and Dangila respectively. For Anjeni and Temcha watershed the observed average maximum temperature have 23.36 °C and 24.5 °C and minimum temperature 9.15 °C and 10.69 °C respectively. Like the precipitation records, CORDEX-Africa model outputs generally had little variation between the annual mean maximum temperature 23.47 °C and 22.4 °C, and mean minimum temperature 13.96 °C and 12.35 °C of grid. Hence the CORDEX- Africa model datasets present different historical means and distributions from the observed dataset; the decision to perform bias correction was inevitable. Due to these reason relatively simple bias correction method could be used to shift and adjust the data to the observed mean and standard deviation.

4.2 Projected Changes in Climate Variables

Precipitation

The projected average monthly precipitation indicated a decreasing trend from march–September and increasing from October–February except during the month of December, from the base line period for all three catchments. In Anjeni watershed, the projected average monthly precipitation change ranging from (−25.4% to 92.2%), (−69.4% to 103.1%) and (−39.9% to 34.3%) in 2030s, 2060s and 2090s for RCP2.6 respectively. The maximum change was observed in month of November (92.2%) in 2030s and October (103.1% and 34.3%) in 2060s and 2090s. Similarly, for RCP8.5, the projected average monthly precipitation change ranges from (−51.1% to 79.2%), (−64.1% to 76.8%) and (−84.2% to 92.7%) in 2030s, 2060s and 2090s respectively. The maximum change was observed in month of February (79.2%), November (76.8%) and December (92.3%) in 2030s, 2060s and 2090s respectively. For both RCPs the increment of precipitation change was observed mostly in dry months (October–February). However, the reduction was observed in wet months (March–September) (Fig. 2a).

In Temcha watershed, the projected average monthly precipitation change ranging from (−30.47% to 64.26%), (−65.53% to 48.35%) and (−31.05% to 68.8%) in 2030s, 2060s and 2090s for RCP2.6 respectively. The maximum change was observed in month of January (64.26%) in 2060s and October (48.35% and 68.8%) in 2030s and 2090s. Similarly, for RCP8.5, the projected average monthly precipitation change ranges from (−48.2% to 61.1%), (−1.95% to 36.5%) and (−70.4% to 65.8%) in 2030s, 2060s and 2090s respectively. The maximum change was observed in month of February (61.1%) in 2060s January (36.5%) and (65.8%) in 2030s and 2090s respectively. For both RCPs the increment of precipitation change was observed mostly in dry months (October–February). However, the reduction was observed in wet months (march–September) (Fig. 2b).

In Gilgel Abbay watershed, the projected average monthly precipitation change ranging from (−2.5% to 42.8%), (−40.4% to 106.8%) and (−50% to128%) in 2030s, 2060s and 2090s for RCP2.6 respectively. The maximum change was observed in month of March (42.8%, 106.8% and 128.6%) in 2030s, 2060s and 2090s. Similarly, for RCP8.5, the projected average monthly precipitation change ranges from (−43.6% to 156.0%), (−65.7% to 103.6%) and (−68.3% to132.9%) in 2030s, 2060s and 2090s respectively. The maximum change was observed in month of February (156.6%), March (103.6%) and November (132.9%) in 2030s, 2060s and 2090s respectively. For both RCPs the increment of monthly precipitation change was observed mostly in dry months (October−February). However, the reduction was observed in wet months (march–September) (Fig. 2c). In general, in main rainy season (June to September) the rainfall exhibits decreasing scenario from base line period in RCP2.6 and RCP8.5 in all watersheds and future time horizons (Fig. 2). In general, the projected monthly change of future precipitation decreases in the month of March to September.

The average seasonal precipitation result indicated that in the future, the precipitation decreases in summer and spring in both RCP2.6 and RCP8.5. However, it increases in winter and autumn. The average annual precipitations presented in Table 1 and Fig. 3 shows, over each watershed the precipitation decreases in the future period for both RCPs. The maximum annual change was observed in 2090s for both RCPs and all watersheds.

The projected mean monthly precipitation shows similar pattern with the work of [21] which, describes the impact of climate change on Gilgel Abbay watershed using A2 and B2 scenarios. Gebre and Ludwig [22] indicated in their studies the mean monthly precipitation increased in a positive direction particularly in August, September, and October under both in 2030s and 2070s using both scenarios. A 24% increment in precipitation projection in the late 21st century (2070–2099) was reported by [6] using 11 GCMs, while [7] reported insignificant precipitation change by using 17 GCMs in Blue Nile basin. Conway [23] and [3] also indicated that there is large inter-model difference in the detail of rainfall changes over Ethiopia. These inter-model differences in projection of future precipitation is due to the diversity of African climates, high rain fall variability, very sparse observational network makes the prediction difficult at sub regional and local scales. This study shows the projected precipitation for the future period decrease in the main rainy season (June–September) as compared to base period but, the monthly magnitude of rain fall was high from June to September, due to the summer monsoon climate which brings atmospheric moisture into the basin, leading to large amounts of rainfall during the wet season. Generally, the variation of the projected future precipitation for the future period in the Upper Blue Nile basin is due to the variation of GCM model, scenarios used downscaling and bias correction methods, variability of the precipitation in the basin and limited and very sparse observational network availability.

Projected Maximum Temperature
The projected average monthly maximum temperature significantly increases in future periods in both RCPs scenarios. In Anjeni watershed, the maximum change in maximum

Table 1. Shows the change in percentage of projected annual average precipitation

Catchment	Factor	Observed	Projected					
			RCP2.6			RCP8.5		
			2030s	2060s	2090s	2030s	2060s	2090s
Anjeni	AARF(mm)	1608.3	1567.3	1478.1	1396.3	1378.5	1345.1	1114.0
	R^2		0.91	0.89	0.94	0.93	0.92	0.86
	Change (%)		−2.55	−8.10	−13.18	−14.29	−16.36	−30.74
Gilgel Abbay	AARF(mm)	1970.0	1793.0	1812.0	1758.5	1764.4	1717.8	1539.1
	R^2		0.93	0.92	0.89	0.83	0.82	0.76
	Change (%)		−8.98	−8.02	−10.73	−10.44	−12.80	−21.88
Temcha	AARF(mm)	1393.1	1335.9	1288.3	1284.2	1216.2	1251.2	1089.0
	R^2		0.94	0.94	0.95	0.95	0.93	0.91
	Change (%)		−4.10	−7.52	−7.81	−12.70	−10.19	−21.83

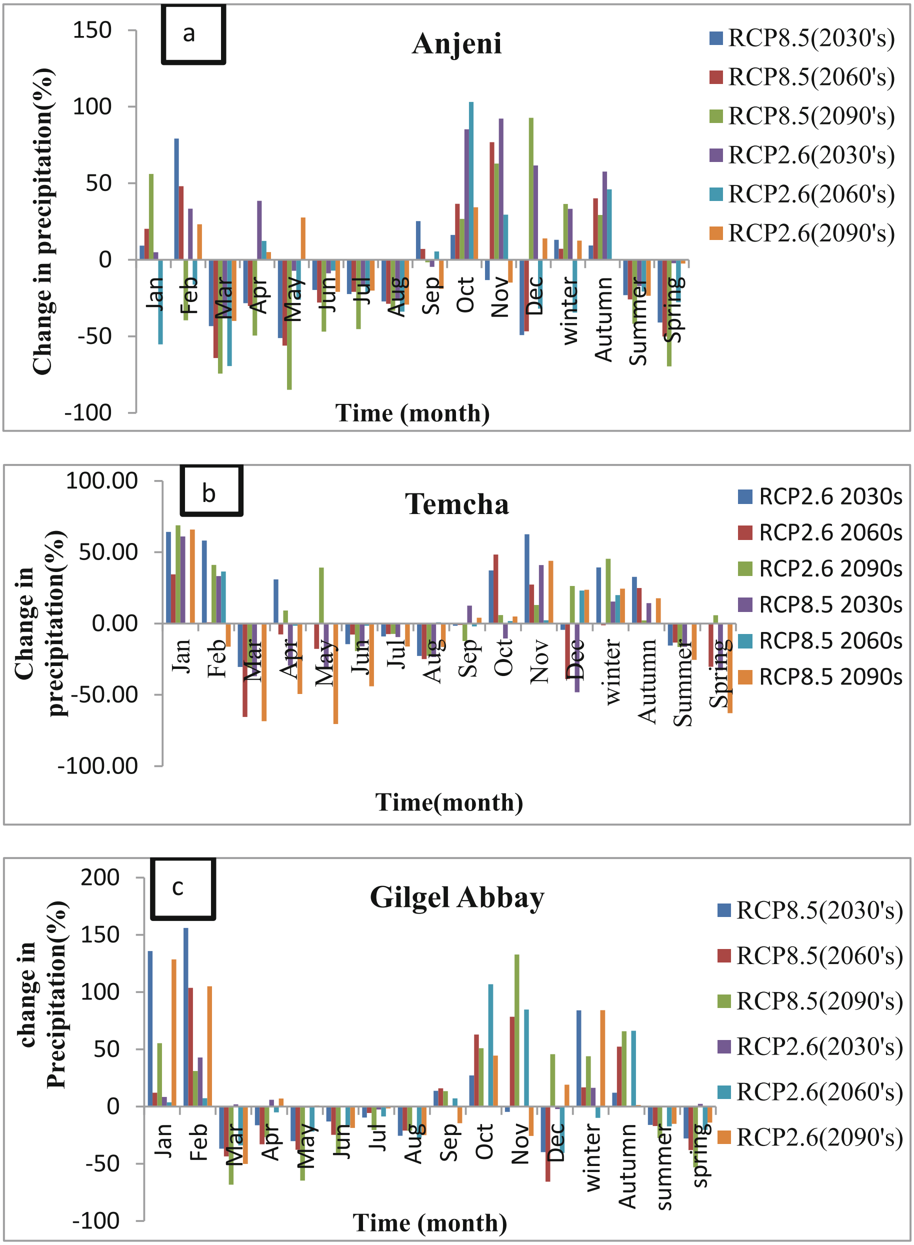

Fig. 2. Relative percentage change of average monthly and seasonal precipitation for 2030s. 2060s and 2090s as compared to the base line period

temperature was observed in January (7.03 °C, 7.22 °C and 8.2 °C) in 2030s, 2060s and 2090s for RCP8.5 respectively. Similarly, for RCP2.6 the maximum change was observed in January (6.8 °C, 7.2 °C, and 6.4 °C) in 2030s, 2060s and 2090s respectively.

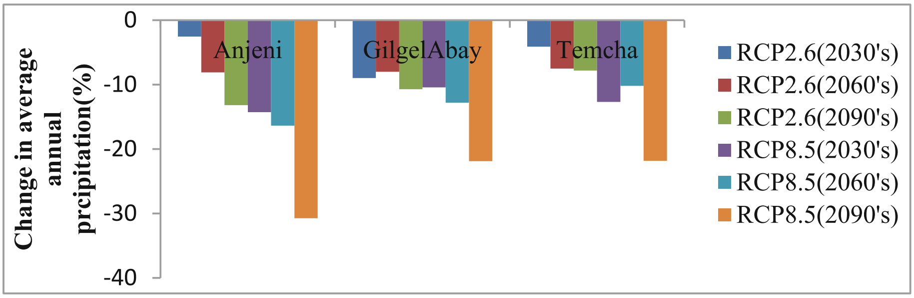

Fig. 3. Relative changes in average annual precipitation on Anjeni, Temcha and Gilgel Abbay watersheds based on RCP2.6 and RCP8.5 for 2030s, 2060s and 2090s as compared to the base period

The minimum change in maximum temperature was observed in July (0.2 °C) in 2030s RCP2.6 (Fig. 4a). Annually, the change of maximum temperature varies from (1.82 °C to 2 °C), (2.9 °C to 3.2 °C) and (5.24 °C to 5.7 °C) in 20305, 2060s and 2090s for RCP8.5. Similarly, for RCP2.6 the change varies from (1.28 °C to 1.42 °C), (1.52 to 1.66 °C) and (1.52 °C to 1.69 °C) in 2030s, 2060s and 2090s respectively.

For Temcha watershed, the maximum change of maximum temperature was observed in January (7.02 °C, 7.4 °C and 7.27 °C) in 2030s, 2060s and 2090s for RCP2.6 respectively. For RCP2.6 the change was observed in January (7.22 °C, 8.4 °C and 10.4 °C) in 2030s, 2060s and 2090s respectively. The minimum change was observed in July in 2030s and 2090s and December in 2060s for RCP2.6 (Fig. 4b). Annually, the change of maximum temperature varies from (1.27 °C to 1.43 °C), (1.51 °C to 1.67 °C) and (1.51 °C to 1.68 °C) in 2030s, 2060s and 2090s for RCP2.6 respectively. Similarly, for RCP8.5 the change varies from (1.82 °C to 2.0 °C), (2.94 °C to 3.22 °C) and (5.24 °C to 5.7 °C) in 2030s, 2060s and 2090s respectively.

For Gilgel Abbay watershed, the maximum change of maximum temperature was observed in January (7.4 °C, 7.7 °C and 7.6 °C) in 2030s, 2060s and 2090s for RCP2.6 respectively. For RCP8.5 the change was observed in January (7.6 °C, 8.7 °C and 10.78 °C) in 2030s, 2060s and 2090s respectively. The minimum change was observed in July in 2030s, August in 2090s and December in 2060s for both RCP2.6 and RCP8.5 (Fig. 4c). Annually, the change of maximum temperature varies from (1.34 °C to 1.48 °C), (1.41 °C to 1.59 °C) and (1.45 °C to 1.63 °C) in 2030s, 2060s and 2090s for RCP2.6 respectively. Similarly, for RCP8.5 the change varies from (1.78 °C to 2.01 °C), (2.86 °C to 3.23 °C) and (5.17 °C to 5.75 °C) in 2030s, 2060s and 2090s respectively.

The change in maximum temperature in dry season was higher than wet season in all future time horizons for both RCP2.6 and RCP8.5 in all watersheds (Fig. 4a–c). This is due to in wet season peak temperatures reduced because of rainfall, cloudy conditions and energy use for evapotranspiration [23]. In all Projection periods the magnitude is higher for the higher emission scenarios of RCP8.5 than for the low emission scenarios of RCP2.6. The projected maximum temperature in all time horizons was within the range projected by IPCC which indicate the average temperature will be rise 1.4–5.8 °C towards the end of the 21st century.

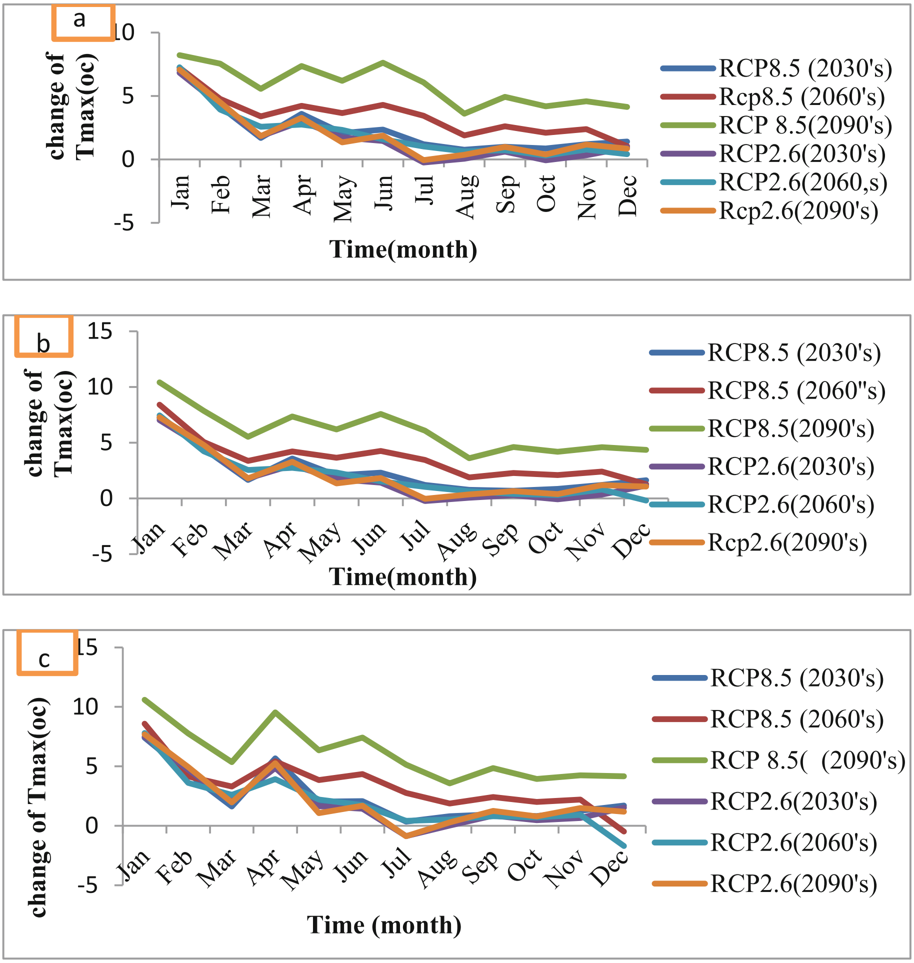

Fig. 4. Projected change in mean maximum temperature at (a) Anjeni (b) Temcha (c) Gilgel Abbay, watershed for 2030s, 2060s and 2090s time windows under RCP 2.6 and RCP8.5.

Projected Minimum Temperature

The minimum temperature showed an increasing trend in all three of future time horizons. In Anjeni watershed, the maximum change in minimum temperature was observed in January (4.9 °C, 5.32 °C and 5.14 °C) in 2030s, 2060s and 2090s for RCP2.6 respectively. Similarly, for RCP8.5 the maximum change was observed in January (3.7 °C, 4.92 °C, and 7.37 °C) in 2030s, 2060s and 2090s respectively. The minimum change in minimum temperature was observed in July (0.02 °C) in 2030s RCP2.6 (Fig. 5a). Annually, the change of minimum temperature varies from (1.32 °C to 1.38 °C), (1.53 °C to 1.62 °C) and 1.55 °C to 1.62 °C) in 2030s, 2060s and 2090s for RCP2.6. Similarly, for RCP8.5 the change varies from (1.46 °C to 1.59 °C), (2.93 to 3.17 °C) and (5.14 °C to 5.55 °C) in 2030s, 2060s and 2090s respectively.

For Temcha watershed, the maximum change of minimum temperature was observed in January (3.12 °C, 3.5 °C and 3.36 °C) in 2030s, 2060s and 2090s for RCP2.6 respectively. For RCP8.5 the change was observed in January (3.27 °C, 4.82 °C and 7.26 °C) in 2030s, 2060s and 2090s respectively. The minimum change was observed in July in 2030s and 2060s and December in 2090s for RCP2.6 (Fig. 5b). Annually, the change of minimum temperature varies from (1.22 °C to 1.34 °C), (1.46 °C to 1.6 °C) and (1.4 °C to 1.5 °C) in 2030s, 2060s and 2090s for RCP2.6 respectively. Similarly, for RCP8.5 the change varies from (1.46 °C to 1.59 °C), (2.94 °C to 3.17 °C) and 5.14 °C to 5.55 °C) in 2030s, 2060s and 2090s respectively.

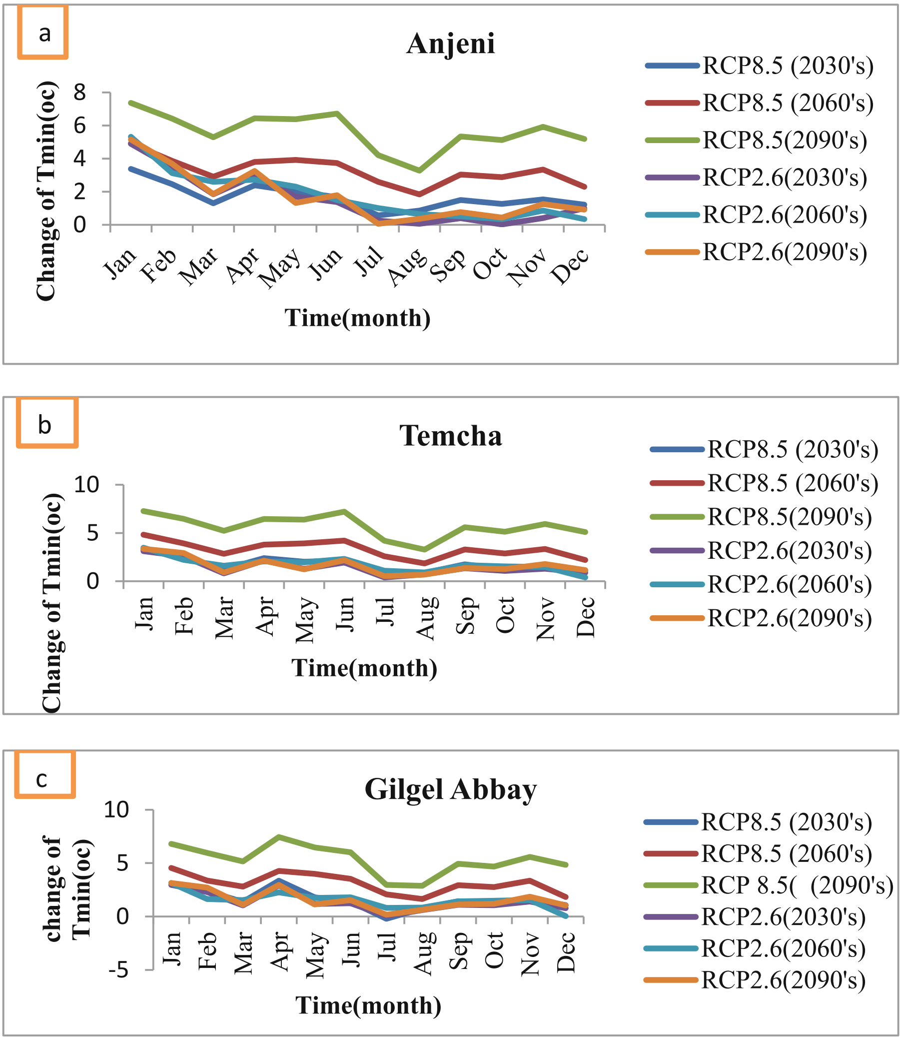

Fig. 5. Projected changes in mean minimum temperature at (a) Anjeni (b) Temcha (c) GilgelAbbay watershed for 2030s, 2060s and 2090s time windows under RCP2.6 and RCP8.5

For Gilgel Abbay watershed, the maximum change of minimum temperature was observed in January (3.1 °C, 3.18 °C and 4.16 °C) in 2030s, 2060s and 2090s for RCP2.6 respectively. For RCP8.5 the change was observed in January (3.25 °C, 4.6 °C and 6.8 °C) in 2030s, 2060s and 2090s respectively. The minimum change was observed in July in 2030s, and 2090s and December in 2060s for both RCP2.6 and RCP8.5 (Fig. 5c). Annually the change of minimum temperature varies from (1.23 °C to 1.34 °C), (1.35 °C to 1.5 °C) and (1.35 °C to 1.5 °C) in 2030s, 2060s and 2090s for RCP2.6 respectively. Similarly, for RCP8.5 the change varies from (1.43 °C to 1.56 °C), (2.83 °C to 3.09 °C) and 4.84 °C to 5.25 °C) in 2030s, 2060s and 2090s respectively. The minimum relative change of temperature is observed in July in all climate periods and emission scenarios except in 2060s in RCP2.6 which occurs in December. The projected minimum temperature increases an average of 1.47 °C and 1.7 °C, over the short-term period 2030s, 1.6 °C and 3.7 °C over midterm period 2060s and 1.68 °C and 5.6 °C over the long-term period 2090s in both RCP2.6 and RCP8.5 respectively for all three watersheds (Fig. 5a–c).

Potential Evapotranspiration

The projected change in average monthly potential evapotranspiration indicated an increasing for RCP2.6 and RCP8.5 for all watersheds. In Anjeni watershed, the maximum change in potential evapotranspiration was observed in January for (51.6%, 38 mm/month), (57.1%, 42 mm/month) and (63.3%, 46.6 mm/month) in 2030s, 2060s and 2090s for RCP8.5 respectively. Similarly, for RCP2.6 the change was observed in January (53.6%, 39.4 mm/month), (57.3%, 42.2 mm/month) and (54.9%, 40.4 mm/month) in 2030s, 2060s and 2090s respectively. The minimum evapotranspiration change was observed in August (0.25%, 0.13 mm/month), (6.3%, 2.8 mm/month) and (15%, 6.8 mm/month) in 2030s, 2060s and 2090s for RCP8.5 respectively. In RCP2.6 the minimum change was observed in August and September (less than 1.68%, 0.9 mm/month) in all future time horizons. Annually, the change of potential evapotranspiration varies from (92.6 to 111.5 mm/year), (102.4 to 119.2 mm/year) and (106 to 122.7 mm/year) in 2030s, 2060s and 2090s for RCP2.6. Similarly, for RCP8.5 the change varies from (116.2 to 133.6 mm/year), (174.7 to203.44 mm/year) and (315.4 to 361mm/year) in 2030s, 2060s and 2090s respectively (Fig. 6).

In Temcha watershed, the maximum change in potential evapotranspiration was observed in January (49.6%, 60.45 mm/month), (50.89%, 61.94 mm/month) and (53.1%, 64.65 mm/month) in 2030s, 2060s and 2090s for RCP2.6 respectively. Similarly for RCP8.5 the change was observed in January (48%, 58.5 mm/month), (53.34%, 64.9 mm/month) and (59.47%, 72.47 mm/month) in 2030s, 2060s and 2090s respectively. The minimum evapotranspiration change was observed in August (0.39%, 0.26 mm/month), (7.4%, 5.07 mm/month) and (17.3%, 11.72 mm/month) in 2030s, 2060s and 2090s for RCP8.5 respectively. In RCP2.6 the minimum change was observed in August and December (less than 3%, 3.8 mm/month) in all future time horizons (Fig. 6). Annually, the change of potential evapotranspiration varies from (96.2 to113.2 mm/year), (101.99 to 122.9 mm/year) and (106.9 to 127.3 mm/year) in 2030s, 2060s and 2090s for RCP2.6. Similarly, for RCP8.5 the change varies from (117.8 to 137.6 mm/year), (181 to 209 mm/year) and (326.8 to 376 mm/year) in 2030s, 2060s and 2090s respectively.

In Gilgel Abbay watershed, the maximum change in potential evapotranspiration was observed in January (53.75%, 56.6 mm/month), (57.1%, 60.2 mm/month) and (55%, 58 mm/month) in 2030s, 2060s and 2090s for RCP2.6 respectively. Similarly, for RCP8.5 the change was observed in January (49.9%, 52.6 mm/month), (49.4%, 52.04 mm/month) and (63.4%, 66.8 mm/month) in 2030s, 2060s and 2090s respectively. The minimum evapotranspiration change was observed in August (0.78%, 0.58 mm/month) and (13.9%, 10.31 mm/month) in 2006s and 2090s for RCP8.5 respectively. In 2030s the minimum change was observed in September (0.6%, 0.65 mm/month) for RCP8.5. In RCP2.6 the minimum change was observed in September, November and October (less than 1.2%, 1.32 mm/month) in 2030s, 2060s and 2090s respectively (Fig. 8). Annually the change of potential evapotranspiration varies from (105.8 to 117.7 mm/year), (102.8 to 126 mm/year) and (105.7 to 127.5 mm/year) in 2030s, 2060s and 2090s for RCP2.6. Similarly, for RCP8.5 the change varies from (113.1 to 130.8 mm/year), (112.6 to 130.8 mm/year) and (315.2 to 367.5 mm/year) in 2030s, 2060s and 2090s respectively.

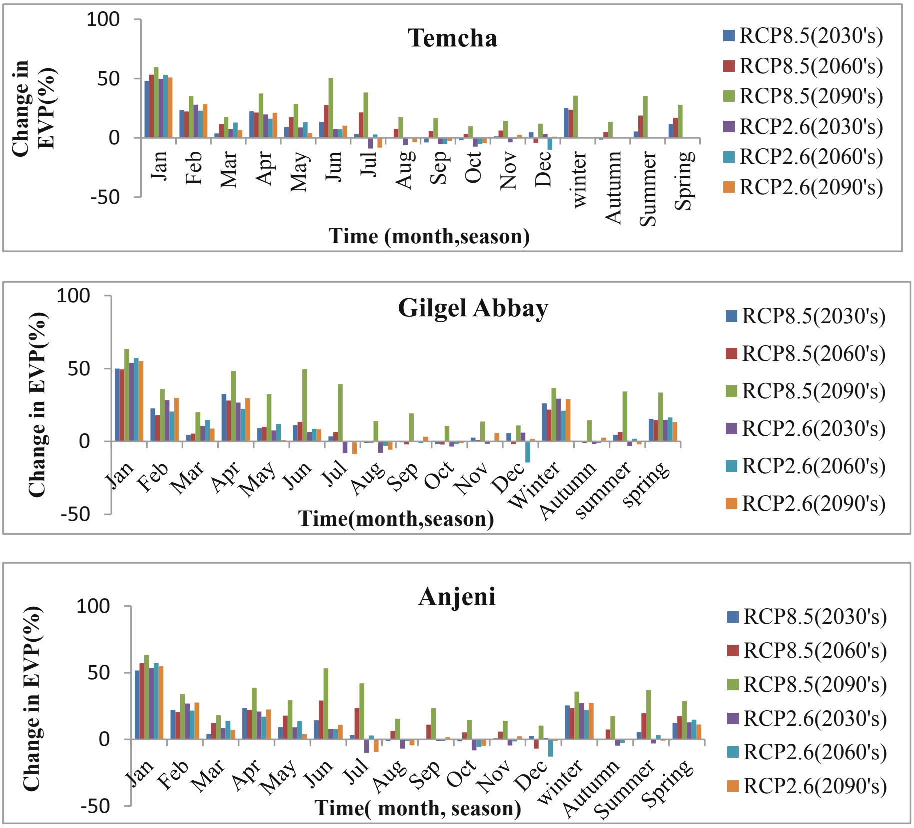

Fig. 6. Relative percentage change of average monthly and seasonal potential evapotranspiration for 2030s, 2060s and 2090s as compared to the base line period

In all-time windows the reduction of percentage change is observed in the months of July to October except in 2060s and 2090s for RCP8.5. The projected average seasonal potential evapotranspiration increases in all seasons for both emission scenarios. Generally, a positive potential evaporation change resulted both seasonally and annually for all future time horizons as compared to the base line period (Fig. 6). The increment of evapotranspiration is due to increment of temperature [23]. The decreasing of rainfall and increasing of temperature result the increasing of evapotranspiration. This also results decrement of stream flow.

4.3 Hydrological Modeling of the Watersheds

The hydrology of the watershed was modeled by using the parameter efficient semi- distributed watershed (PED-W) model. The PED-W model were calibrated manually, first by fitting the Discharge followed by calibrating the shape of the hydrograph from 1990 to 2000 for Gilgel Abbay, 1986 to 1994 for Temcha and Anjeni. The calibrated model was validated from 2001 to 2005, 1996 to 1998 and 1995–1998 for three of watersheds respectively. The discharge was simulated at a daily time step with NSE of 0.78 and 0.74 for Gilgel Abbay, 0.60 and 0.56 for Temcha, and 0.76 and 0.5 for Anjeni watershed during calibration and validation period respectively. On the monthly time scale the model was simulated with NSE of 0.91 and 0.89 for Gilgel Abbay, 0.91 and 0.89 for Temcha and 0.91 and 0.88 for Anjeni watershed for calibration and validation respectively. The initial points of parameters used for calibration and validation were dependent up on the value of the previous studies of PED-W model on the upper Blue Nile basin by [18] and [24]. Manually changing the parameters until the observed and predicted discharge hydrograph fits. The calibration and validation result of Gilgel Abbay was consistently in the range with earlier studies of PED-W discharge simulation for Ethiopian high lands watershed by [25]. In Anjeni and Temcha watershed the NSE and R^2 results are consistent with previous similar studies ([18, 25, 26] in range of ($0.53 < NSE < 0.78$) at daily time step, during calibration and validation periods (Table 2). The difference of parameters in values and model performance indicators from the previous studies in the same area might be due to recorded length of observed discharge in calibration and validation. During calibration and validation the PED-W model parameters of the fractional

Table 2. Shows the calibration and validation performance of the PED –W model

Watershed	Description	Daily			Monthly		
		R^2	NSE	RMSE	R^2	NSE	RMSE
Gilgel Abbay	Calibration	0.80	0.78	0.49	0.94	0.91	0.31
	Validation	0.78	0.74	0.53	0.93	0.89	0.33
Temcha	Calibration	0.61	0.60	0.63	0.92	0.9	0.30
	Validation	0.60	0.56	0.67	0.86	0.82	0.43
Anjeni	Calibration	0.78	0.76	0.49	0.93	0.91	0.30
	Validation	0.53	0.5	0.71	0.93	0.88	0.34

areas, the half-life of the base flow, and duration of the interflow after a rainstorm and Maximum soil storage for base flow (Bsmax) are sensitive for the forecasting of stream discharge.

4.4 The Impacts of Climate Change on Stream Flow

The projected change of mean monthly discharge for the three future time horizons: 2030s, 2060s and 2090s has indicated an increasing from October–February and decreasing from March–September except, Temcha watershed in RCP2.6 in May in 2060s (Fig. 7). The simulated stream flow with both scenarios from bias corrected climate model indicated a reduction and increment of discharge in the watersheds. This was directly related to the reduction and increment in precipitation, but there was also reduction of precipitation and increment in potential evapotranspiration in a season, these factors are anticipated to decrease the runoff on that season, however there was an increment of runoff in winter and autumn seasons from the base period.

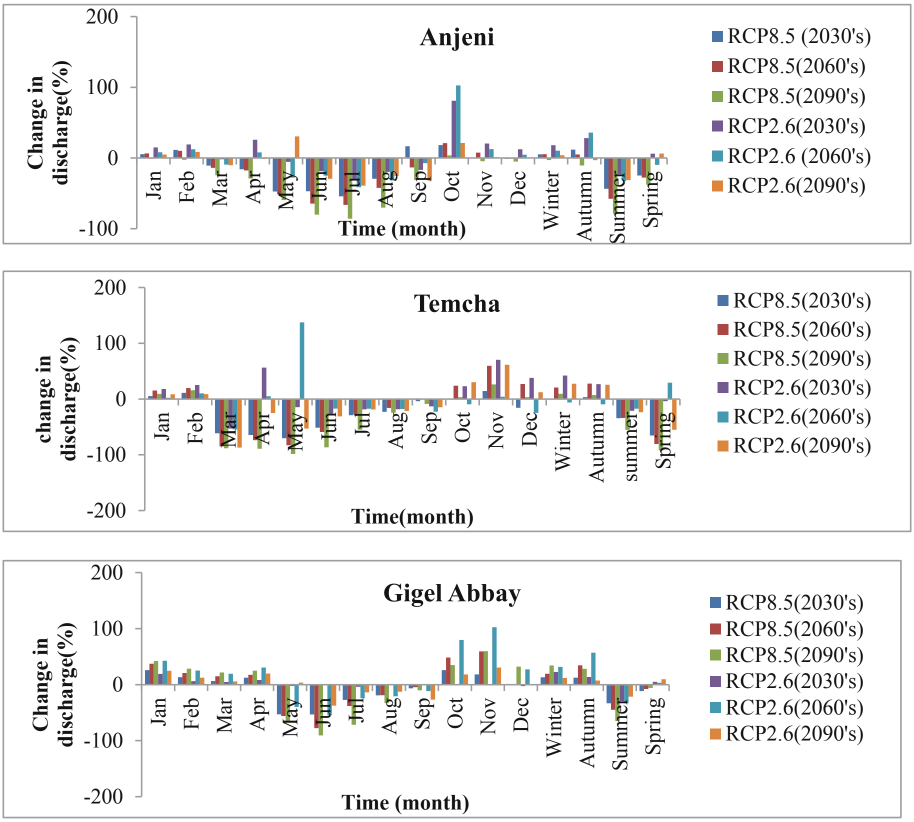

Fig. 7. Relative percentage change in mean monthly runoff for 2030s, 2060s and 2090s under RCP2.6 and RCP8.5 scenarios as compared to the baseline period.

In 2090s even though the change of precipitation with respect to the base period for this future time series has the same value in range with the first future time series 2030s and 2060s, high reduction stream flow was anticipated in RCP2.6 in Gilgel Abbay watershed because there is high increment of potential Evapotranspiration. In this period, the evapotranspiration have high increment rather than the first future time series (2030s) and (2060s). This increment of evapotranspiration results high decrements of runoff in this period.

In Anjeni watershed, the maximum change of increment of stream flow was observed in October (81%, 0.55 m^3/s), (102.64%, 0.74 m^3/s) in 2030s and 2060s for RCP2.6. In 2090s, the maximum change was observed in May (30.6%, 0.03 m^3/s). The maximum change of decrement of stream flow was observed in July (0.58 m^3/s, 0.79 m^3/s and 0.75 m^3/s) in 2030s, 2060s and 2090s respectively. Similarly, for RCP8.5, the maximum change was observed in October (18.25%, 0.12 m^3/s), (21.1%, 0.14 m^3/s) and (3.76%, 0.025 m^3/s) in 2030s, 2060s and 2090s respectively. The maximum reduction was observed in July in all time future.

In Temcha watershed, the maximum change of increment was observed in October (70.4%, 49 m^3/s) and (61.4%, 43.3 m^3/s) in 2030s and 2090s for RCP2.6. In 2060s the change was observed in May (137.58%, 26 m^3/s). Similarly for RCP8.5 the maximum change was observed in November (14.5%, 10.2 m^3/s), (59.6%, 42 m^3/s) and (26.4%, 18.6 m^3/s) in 2030s, 2060s and 2090s respectively. The maximum reduction was observed in May (98.4%, 18.6 m^3/s) in 2090s.

In Gilgel Abbay watershed, the maximum change of increment was observed in November (102.64%, 25 m^3/s) and (30.5%, 7.7 m^3/s) in 2060s and 2090s for RCP2.6 respectively. In 2030s, the change was observed in January (19.2%, 0.98 m^3/s). Similarly, for RCP8.5 the maximum change was observed in November (59.2%, 15 m^3/s) in both 2060s and 2090s. In 2030s also the change was observed in October (25.98%, 19.6 m^3/s). The maximum reduction was observed in June (90.7%, 40 m^3/s) in 2090s.

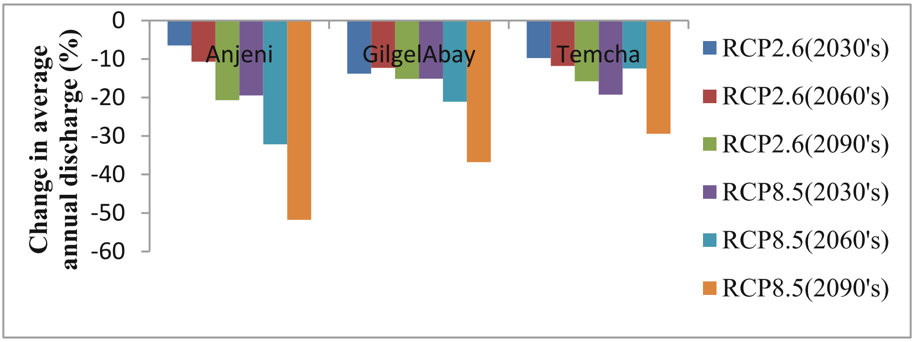

Fig. 8. Relative percentage change in mean annual runoff for 2030s, 2060s and 2090s under RCP2.6 and RCP8.5 scenarios as compared to the baseline period

Figure 7 indicated all watersheds have reduced value of Streamflow in all future time horizon 2030s, 2060s and 2090s in summer and spring season except RCP2.6 in all future time in spring season Gilgel Abbay (3.37%, 5.06% and 9.75%), Anjeni (6.16 in

2030s and in 2090s 6.4%), Temcha (29.37% in 2060s). In winter and autumn season, the projected Streamflow showed increment in all time horizons except RCP2.6 in 2030s for Temcha and RCP8.5, 2090s for Anjeni watershed.

The average annual stream flow showed a decreasing in the future time horizon for both RCPs in all three watersheds. The average annual flow shows maximum reduction of 51.78% at Anjeni, 36.77% at Gilgel Abbay and 29.40% at Temcha watershed in 2090s (Fig. 8).

4.5 The Impacts of Climate Change on the Stream Flow Events

Maximum Flow Analysis Using Annual Maximum Method

The maximum flow analysis was carried out using annual maximum method. This method evaluates the maximum annual flow by selecting the maximum flow from a year. The change of maximum annual flow for the first future time series 2030 s indicated an increasing in RCP2.6 scenario for Anjeni, Gilgel Abbay and Temcha catchments which have more than 4.5% change with respect to the base period maximum flow (1986–2005). However, in RCP8.5 scenario Gilgel Abbay and Temcha catchments show decrement mainly which have reduction more than 4.98%. In Anjeni watershed, the highest increment was (81.07%) for RCP2.6. In Gilgel Abbay watershed the highest reduction (10.15%) was observed for RCP8.5 for the first future time series with respect to the base period maximum annual flow (Table 3).

Table 3. Change of high stream flow for future periods in two scenarios as compared to base period

Watershed	RCP2.6							RCP8.5					
	Annual maximum flow				Percentage change			Annual maximum flow			Percentage change		
	Base period	2030s	2060s	2090s	2030s	2060s	2090s	2030s	2060s	2090s	2030s	2060s	2090s
Anjeni	0.3	0.5	0.5	0.3	81.1	101.4	19.0	0.3	0.3	0.3	28.9	19.8	7.4
Gilgel Abbay	388.5	406.0	486.2	434.0	4.5	25.2	11.7	349.0	406.0	379.3	−10.2	4.5	−2.4
Temcha	68.2	77.9	68.9	62.2	14.1	1.0	−8.9	64.8	75.2	65.0	−5.0	10.2	−4.8

For the second future time horizon 2060s, the percentage change of maximum annual flow showed an increment in all catchments in both RCP scenarios. The maximum increment (101.4%) was seen for Anjeni watershed in Rcp2.6. The change of maximum annual flow in the long -term future time horizon 2090s indicated an increasing for Anjeni and Gilgel Abbay watershed in RCP2.6. Whereas in RCP8.5 only increase for Anjeni watershed. For Temcha watershed, the maximum decrement was showed in both RCPs. A maximum change in 2090s was observed in Anjeni (7.43%) and Temcha (−8.89%) watersheds (Table 3). For all catchments the percentage change of maximum annual flow indicated an increment in RCP2.6 for all future time horizons except, 2090 s for Temcha. In RCP8.5 scenario for Gilgel Abbay and Temcha watershed indicated a decrement for 2030 and 2090s. However, Gilgel Abbay, and Temcha catchments indicated an increment for 2060s future time horizon and Anjeni for all future time horizons. In general, the increasing of high flow extremes in the future causes flooding and ground water reduction.

Maximum Flow Analysis Using Flow Duration Curve

For 5% probability (Q_5) of exceedance, the percentage change of maximum daily flow in 2030 s was changed from −2% to 36.1% in RCP2.6 scenario for Anjeni, Gilgel Abbay and Temcha catchments with respect to the base period flow (1986–2005). However in RCP8.5 scenario all catchments indicated decrement mainly which have reduction less than 10.2% (Table 4). For the future time horizon 2060s and 2090s the 5% probability of exceedance change from (−1.5% to −56.4%) for both RCPs. The maximum change of increment was observed at (Gilgel Abbay 36.1%) in 2030s and reduction at (Temcha 56.4%) in 2090s. Generally the extreme high flow (Q_5) changed in wide range from (−56.4% to 36.1%) (Table 4).

Table 4. Change of high stream flow (Q5) for future periods under two scenarios as compared to base period

Watershed	RCP2.6			RCP8.5		
	Percentage change			Percentage change		
	2030s	2060s	2090s	2030s	2060s	2090s
Anjeni	−2.0	7.4	8.2	−2.9	−13.1	−27.9
Gilgel Abbay	36.1	−1.5	−8.9	−10.2	−15.8	−40.0
Temcha	0.0	0.0	0.0	0.0	0.0	−56.4

This study supports the studies [27–29] which showed wide projections, from (1%–10%) probability of exceedance, with an overall changes in high stream flows was (−43% to 60%), prompting a reduction in drought events for the 2020 s, 2050 s and 2080 s at the Upper Blue Nile basin scale. Also there is little variation in range from the above studies, due to scale of watersheds, climate model used, emission scenario differences and hydrological model.

Low Flow Analysis Using Flow Duration Curve

Climate change affects both the high flows and low flows owing to variability in the precipitation and temperature. In this investigation, to describe low flow conditions in the stream a 95% exceedance probability was considered. The effect at 95% exceedance probability in 2030s, 2060s and 2090s the low flow indicated a decrement in both RCP scenarios for all catchments except RCP2.6 for Anjeni catchment with respect to the baseline situation. Table 5 and Fig. 9(a–c) indicated that the extreme low flow statistics at 95% exceedance probability decreased in all watersheds and RCPs. The maximum change of low flow was observed at (Temcha −61.7%) watershed in 2090s and the minimum change was at (Anjeni 1.43%) in 2090s (Table 5).

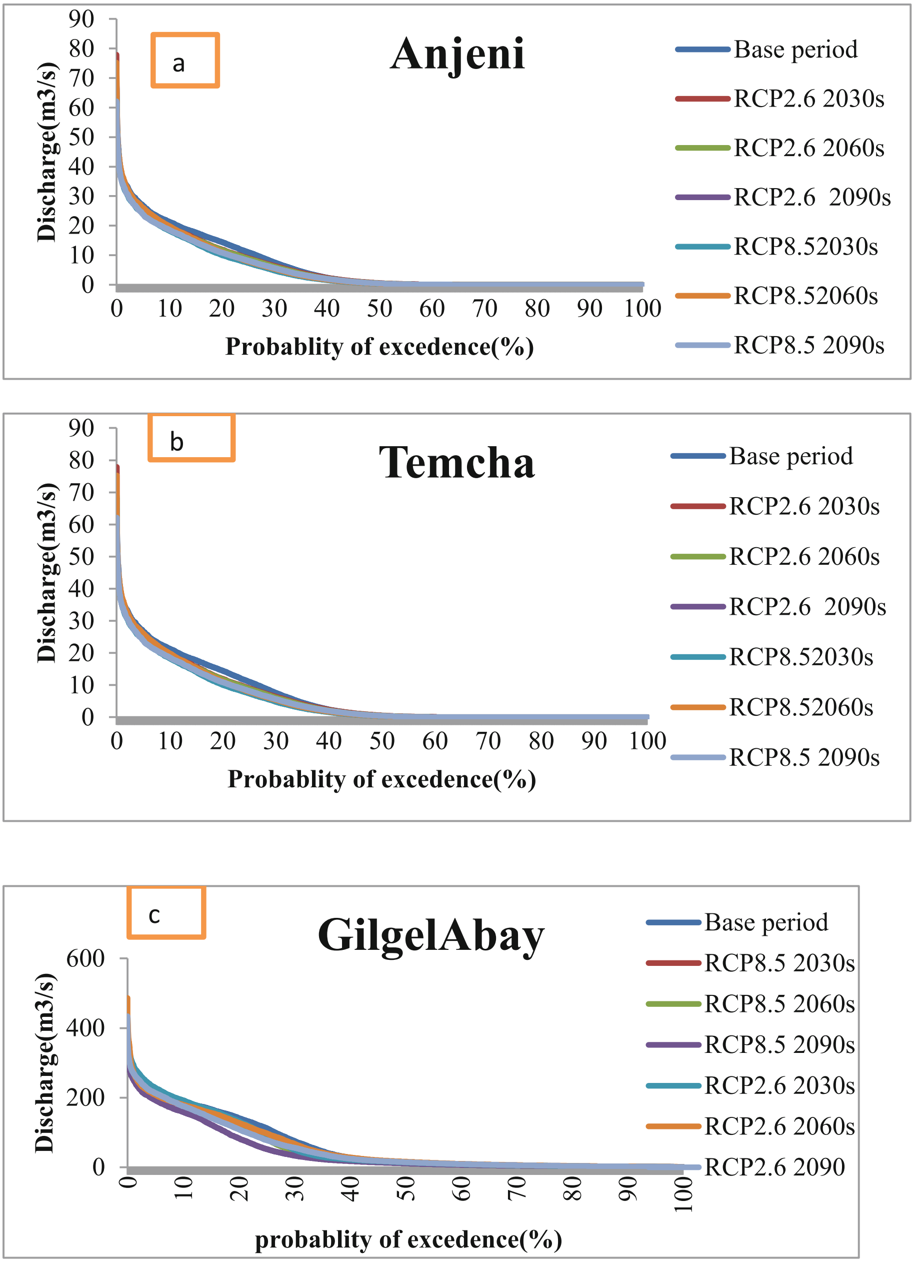

Fig. 9. Flow duration curve for RCP2.6 and RCP8.5 scenario for different time periods (a) Anjeni (b) Temcha (c) Gilgel Abbay

At the yearly scale, statistically significant declines in stream flow are reported by [30], However, [27] indicated an increasing trend in low stream flow statistic (Q_{90})

Table 5. Change of low stream flow (Q95) for future periods under two emission scenarios as compared to base period

Watershed	RCP2.6			RCP8.5		
	Percentage change			Percentage change		
	2030s	2060s	2090s	2030s	2060s	2090s
Anjeni	7.73	3.37	1.43	−7.22	−15.20	−48.44
Gilgel Abbay	−25.92	8.17	−1.04	−9.53	−7.18	−27.47
Temcha	−4.65	−11.25	−31.11	−33.49	−21.93	−61.72

using six GCM with A2 scenario in range of −25% to 60% for the 2050 horizon. Using 17 GCMs with A1B and B1 scenarios for the same 2050s horizon, [11] discover that changes low stream flows vary from −61% to +56%. Similarly, using three GCMs, [31] reported that projections of drought characteristics for future periods do not agree on the direction or magnitude for the Lake Tana sub-basin. However, [10] study on Gilgel Abbay sub basin using hadCM3 model, the low stream flow (Q_{95}) did not show any effects in 2020s, 2050s and 2080s. But Q_{70} flow decrease in 2020s and 2050s and increase for 2080s. This study analyzed the low stream flow Q95 using the Coordinated Regional Climate Downscaling Experiment in Africa (CORDEX Africa) outputs based on RCP2.6 and RCP8.5 scenarios for the future 2030s, 2060s and 2090s time horizon and the result indicated similar trends [10, 11, 27]. The decrement of low flow (Q_{95}) for the future period indicated the availability of water in the watershed for the future will reduced. The reason for this was due to changes in precipitation and temperatures can affect the magnitude and timing of runoff, which in turn affect the frequency and intensity of hydrologic extreme events such as floods and droughts.

5 Conclusions

This study evaluated the impacts of climate change on extreme state of hydrology using the downscaled bias corrected output and Hydrological model simulation approach of PED-W model. So the study reached on the following conclusions. The projected precipitation for the future time horizon increases from October to February and decrease from March to September for both scenarios Rcp2.6 and RCP8.5. For RCP2.6 the monthly maximum increment of precipitation reaches up to 92.2% at Anjeni in 2030s and (106.8% and 128%) at Gilgel Abbay 2060s and 2090s. For RCP8.5, the increment reaches 156%, 103.6% and 132.8% at Gilgel Abbay in 2030s, 2060s and 2090s respectively. The monthly maximum precipitation reduction reaches up to 30.47% and 51.1% for 2030s, 69% and 65.7% for 2060s and 70% and 84.8% for 2090s both in RCP2.6 and RCP8.5 respectively. Seasonally, the projected precipitation increase in winter and autumn, however, it decreases in summer and spring. The average increment reaches a maximum of 84.26% for RCP2.6 and 84.04% for RCP8.5 in Gilgel Abbay watershed. The annual precipitation shows decreasing trend for both RCP2.6 and RCP8.5 scenarios in all watersheds with the maximum decrement of 30.74% at Anjeni towards the end

21st century. The results of the projected monthly, seasonal and annual maximum and minimum temperature indicated an increasing trend in all future time horizons for both RCP2.6 and RCP8.5 scenarios. For RCP2.6 the maximum monthly increment of maximum and minimum temperature was observed in January reaches up to 7.4 °C and 4.9 °C in 2030s, 7.7 °C and 5.32 °C in 2060s and 7.6 °C and 5.14 °C in 2090s respectively. For RCP8.5, the maximum increment of maximum and minimum temperature reaches up to 7.6 °C and 3.7 °C in 2030s, 8.7 °C and 4.92 °C in 2060s and 10.78 °C and 7.37 °C in 2090s. In all projection period the maximum monthly increment was observed at Gilgel Abbay and minimum temperature at Anjeni watershed. The projected average annual maximum temperature changes (1.9, 3.05 and 5.46 °C) in 2030s, 2060s and 2090s for RCP8.5 in all watersheds respectively. For RCP2.6 the maximum change (1.35, 1.59 and 1.6 °C) in 2030s, 2060s and 2090s projection period. The projected annual maximum temperature in all time horizons is with the range projected by IPCC which indicate the average temperature will be rise 1.4–5.8 °C towards the finish of the century. The model performance criterion which was used to evaluate the model result indicates that the daily and monthly Nash and Sutcliffe efficiency criteria (NSE) within the ranges 0.6 to 0.78 and 0.9 to 0.91 during calibration and 0.5 to 0.74 and 0.82 to 0.89 during validation period respectively. The result indicated that the average projected monthly, seasonal and annual stream flow changes mainly corresponding to the change in precipitation except in month of March and April and spring season in Gilgel Abbay catchment which the flow increases even though the precipitation decreases. The maximum reduction of the average monthly flow reaches up to 85.76% at Anjeni, 90.7% at Gilgel abbey and 98.4% at Temcha watershed in 2090s for RCP8.5 and the maximum increment of the average monthly stream flow reaches up to 102.64% at Anjeni and Gilgel abbey and 137.58% at Temcha watershed in 2060s for RCP2.6. The average annual stream flow showed decreasing in the future time horizon for both RCPs in all three watersheds. The average annual flow shows maximum reduction of 51.78% at Anjeni, 36.77% at Gilgel Abbay and 29.40% at Temcha watershed in 2090s. The result indicated that the maximum flow event in both maximum annual and flow duration curve method changes in wide ranges from (−56.4 to 81.1%) in both scenarios for the future time and the minimum flow (Q_{95}) changes from (−61.72% to 8.17%). In general, the results from this study have clearly indicated that there would be variability in rainfall on the monthly and seasonal variation. Besides there would be also increasing trend in temperature and decreasing low flows. This indicates that there would be higher demand of evapotranspiration in dry season which additional water resource developments need to be planned for irrigation to sustain the already fragile food security of the country. Hence the water resource management and planning in the Blue Nile basin should address thesis phenomenon. Therefore, prevention and adaptation strategies in and around these watersheds have to be developed so as to maintain sustainability of available water resources and to prevent extreme events.

References

1. Baede, A.P.M.: The climate system: an overview. In: Climate Change 2001: The Scientific Basis, pp. 38–47 (2001)

2. Cubasch, U., et al.: Projections of future climate change. Climate change 2001: the scientific basis. Contribution of Working Group I to the Third Assessment Report of the Intergovernmental Panel on Climate Change. In: Ding, Y., et al. (eds.), pp. 526–582. Cambridge University Press, New York (2001)
3. Latta, G., Temesgen, H., Adams, D., Barrett, T.: Analysis of potential impacts of climate change on forests of the United States Pacific Northwest. For. Ecol. Manage. **259**, 720–729 (2010)
4. Pachauri, R.K., et al.: Climate change 2014: synthesis report. Contribution of Working Groups I, II and III to the fifth assessment report of the Intergovernmental Panel on Climate Change. IPCC (2014)
5. IPCC (2007). https://scholar.google.com/scholar?hl=en&as_sdt=0%2C5&q=IPCC%2C+2007+&btnG. Accessed 1 Nov 2019
6. Beyene, T., Lettenmaier, D.P., Kabat, P.: Hydrologic impacts of climate change on the Nile River Basin: implications of the 2007 IPCC scenarios. Clim. Change **100**, 433–461 (2010)
7. Elshamy, M., Seierstad, I.A., Sorteberg, A.: Impacts of climate change on Blue Nile flows using bias-corrected GCM scenarios. Hydrol. Earth Syst. Sci. **13**, 551–565 (2009)
8. Kim, U., Kaluarachchi, J.J.: Climate change impacts on water resources in the upper Blue Nile River Basin, Ethiopia 1. JAWRA J. Am. Water Resour. Assoc. **45**, 1361–1378 (2009)
9. Adem, A.A., et al.: Climate change projections in the upper Gilgel Abay River catchment, Blue Nile Basin Ethiopia. In: Melesse, A.M., Abtew, W., Setegn, S.G. (eds.) Nile River Basin, pp. 363–388. Springer, Cham (2014). https://doi.org/10.1007/978-3-319-02720-3_19
10. Dile, Y.T., Berndtsson, R., Setegn, S.G.: Hydrological response to climate change for Gilgel Abay River, in the Lake Tana basin-upper Blue Nile Basin of Ethiopia. PLoS One **8**, e79296 (2013)
11. Taye, M.T., Ntegeka, V., Ogiramoi, N.P., Willems, P.: Assessment of climate change impact on hydrological extremes in two source regions of the Nile River Basin. Hydrol. Earth Syst. Sci. **15**, 209–222 (2011)
12. Ashagre, B.B.: SWAT to identify watershed management options: Anjeni Watershed, Blue Nile Basin, Ethiopia. Ph.D. thesis, Citeseer (2009)
13. Herweg, K., Gebre, M.Y.: Adaptation or adoption? Integrating different perceptions of soil and water conservation in Ethiopia. Local Environ. In: Flury, M., Geiser, U. (eds.) Local Environmental Management in a North-South Perspective: Issues of Participation and Knowledge Management, pp. 181–190. Vdf Hochschulverlag AG ETH Zurich, Zurich (2002)
14. Ludi, E.: Economic Analysis of Soil Conservation: Case Studies from the Highlands of Amhara Region, Ethiopia. Geographica Bernensia, Bern (2004)
15. Anandhi, A., et al.: Examination of change factor methodologies for climate change impact assessment. Water Resour. Res. **47**, W03501 (2011)
16. Penman, H.L.: Natural evaporation from open water, bare soil and grass. Proc. R. Soc. Lond. Ser. Math. Phys. Sci. **193**, 120–145 (1948)
17. Enku, T., Melesse, A.M.: A simple temperature method for the estimation of evapotranspiration. Hydrol. Process. **28**, 2945–2960 (2014)
18. Steenhuis, T.S.: Predicting discharge and sediment for the Abay (Blue Nile) with a simple model. Hydrol. Process. Int. J. **23**, 3728–3737 (2009)
19. Nash, J.E., Sutcliffe, J.V.: River flow forecasting through conceptual models Part I—A discussion of principles. J. Hydrol. **10**, 282–290 (1970)
20. Moriasi, D.N., Arnold, J.G., Van Liew, M.W., Bingner, R.L., Harmel, R.D., Veith, T.L.: Model evaluation guidelines for systematic quantification of accuracy in watershed simulations. Trans. ASABE **50**, 885–900 (2007)
21. Abdo, K.S., Fiseha, B.M., Rientjes, T.H.M., Gieske, A.S.M., Haile, A.T.: Assessment of climate change impacts on the hydrology of Gilgel Abay catchment in Lake Tana basin Ethiopia. Hydrol. Process. Int. J. **23**, 3661–3669 (2009)

22. Gebre, S.L., Ludwig, F.: Hydrological response to climate change of the upper Blue Nile River Basin: based on IPCC fifth assessment report (AR5). J. Climatol. Weather Forecast. **3**, 121 (2015)
23. Conway, D.: From headwater tributaries to international river: observing and adapting to climate variability and change in the Nile basin. Glob. Environ. Change **15**, 99–114 (2005)
24. Collick, A.S., et al.: A simple semi-distributed water balance model for the Ethiopian highlands. Hydrol. Process. Int. J. **23**, 3718–3727 (2009)
25. Tilahun, S.A., et al.: Distributed discharge and sediment concentration predictions in the sub-humid Ethiopian highlands: the Debre Mawi watershed. Hydrol. Process. **29**, 1817–1828 (2015)
26. Moges, M.A., et al.: Suitability of watershed models to predict distributed hydrologic response in the awramba watershed in Lake Tana Basin. Land Degrad. Dev. **28**, 1386–1397 (2017)
27. Kim, U., Kaluarachchi, J.J., Smakhtin, V.U.: Climate change impacts on hydrology and water resources of the upper Blue Nile River Basin, Ethiopia, vol. 126. IWMI, Colombo (2008)
28. Aich, V., et al.: Comparing impacts of climate change on streamflow in four large African River Basins. Hydrol. Earth Syst. Sci. **18**, 1305–1321 (2014)
29. Nawaz, N.R., Bellerby, T., Sayed, M., Elshamy, M.: Blue Nile runoff sensitivity to climate change. Open Hydrol. **4**, 137–151 (2010)
30. Setegn, S.G., Rayner, D., Melesse, A.M., Dargahi, B., Srinivasan, R.: Impact of climate change on the hydroclimatology of Lake Tana Basin, Ethiopia. Water Resour. Res. **47** (2011)
31. Enyew, B.D., Van Lanen, H.A.J., Van Loon, A.F.: Assessment of the impact of climate change on hydrological drought in Lake Tana catchment, Blue Nile basin, Ethiopia. J. Geol. Geosci. **3**, 174 (2014)